

# **3D Fragment Throw Simulation to Determine Fragment Density and Impact on Buildings**

**Principal Author:** Wenshui Gan

**Co-Author:** Jon D. Chrostowski

**Organization:** ACTA Inc.

**Mailing Address:** 2790 Skypark Drive, Suite 310, Torrance, CA 90505

**Phone:** 310-530-1008

**Fax:** 310-530-8383

**Email:** [gan@actainc.com](mailto:gan@actainc.com) & [chrostowski@actainc.com](mailto:chrostowski@actainc.com)

## **ABSTRACT**

HAZX is a software tool for assessing explosive hazards when the Quantity-Distance (Q-D) safe separation requirements are violated. This paper presents the development of DebrisHaz, a sub-module in HAZX for performing detailed, site specific fragmentation hazard analyses. Features of this module include: a) 3D modeling of site terrain and structures; b) random sampling of fragments from a user-specified fragment source; c) computation of fragment trajectories with drag correction; d) physics-based 3D simulation of fragment impact, bounce and roll; e) use of trajectory-normal method for calculating fragment density; f) capability to track fragment impacts with a 3D structure's wall and roof surfaces using collision detection algorithms; g) calculation of the expected number of penetrations into a building. The trajectory calculator has been verified with a range of established computer programs, and the bounce model has been compared against field test data with good agreement. The tool has been used to perform detailed, site-specific fragment risk analyses that account for unique fragmentation characteristics, uneven/non-uniform terrain, and the shielding of people or structures by natural geographical features or by other structures.

## **INTRODUCTION**

Quantity-Distance (Q-D) analysis is usually the first step in the process of gaining explosive site plant approval. If a site plan is in violation of any of the Q-D requirements, additional supplemental hazard/risk analyses may be performed. These supplemental analyses usually take into account more detailed, site specific information that is outside the consideration in a Q-D analysis. Examples of such site specific information include unique fragmentation characteristics, uneven/non-uniform terrain, and the shielding of people by natural geographical features, man-made barriers or by other structures. DebrisHaz, one of the modules in HAZX (Chrostowski, 2010), is a tool developed to perform detailed, site-specific debris hazard analysis.

In a DebrisHaz analysis, 3-dimensional models are built for the terrain and buildings in a graphical user interface. Fragment groups are developed for potential explosion scenarios. Fragments are randomly sampled from the fragment groups; their drag-corrected trajectories are tracked and their impacts with the terrain and buildings are determined. In the case of a terrain impact, the translational and rotational bounce velocities are determined with a physics-based bounce analysis, and the trajectory tracking continues with the new velocities. In the case of a building impact, the potential of wall or roof penetration is evaluated. If the trajectory of a fragment is below the height of a typical person, its contribution to the pseudo trajectory normal (PTN) fragment density is calculated and tallied.

Report Documentation Page				Form Approved OMB No. 0704-0188	
Public reporting burden for the collection of information is estimated to average 1 hour per response, including the time for reviewing instructions, searching existing data sources, gathering and maintaining the data needed, and completing and reviewing the collection of information. Send comments regarding this burden estimate or any other aspect of this collection of information, including suggestions for reducing this burden, to Washington Headquarters Services, Directorate for Information Operations and Reports, 1215 Jefferson Davis Highway, Suite 1204, Arlington VA 22202-4302. Respondents should be aware that notwithstanding any other provision of law, no person shall be subject to a penalty for failing to comply with a collection of information if it does not display a currently valid OMB control number.					
1. REPORT DATE <b>JUL 2010</b>		2. REPORT TYPE <b>N/A</b>		3. DATES COVERED <b>-</b>	
4. TITLE AND SUBTITLE <b>3D Fragment Throw Simulation to Determine Fragment Density and Impact on Buildings</b>				5a. CONTRACT NUMBER	
				5b. GRANT NUMBER	
				5c. PROGRAM ELEMENT NUMBER	
6. AUTHOR(S)				5d. PROJECT NUMBER	
				5e. TASK NUMBER	
				5f. WORK UNIT NUMBER	
7. PERFORMING ORGANIZATION NAME(S) AND ADDRESS(ES) <b>ACTA, Inc. 2790 Skypark Drive, Suite 310, Torrance, CA 90505</b>				8. PERFORMING ORGANIZATION REPORT NUMBER	
9. SPONSORING/MONITORING AGENCY NAME(S) AND ADDRESS(ES)				10. SPONSOR/MONITOR'S ACRONYM(S)	
				11. SPONSOR/MONITOR'S REPORT NUMBER(S)	
12. DISTRIBUTION/AVAILABILITY STATEMENT <b>Approved for public release, distribution unlimited</b>					
13. SUPPLEMENTARY NOTES <b>See also ADM002313. Department of Defense Explosives Safety Board Seminar (34th) held in Portland, Oregon on 13-15 July 2010, The original document contains color images.</b>					
14. ABSTRACT <b>HAZX is a software tool for assessing explosive hazards when the Quantity-Distance (Q-D) safe separation requirements are violated. This paper presents the development of DebrisHaz, a sub-module in HAZX for performing detailed, site specific fragmentation hazard analyses. Features of this module include: a) 3D modeling of site terrain and structures; b) random sampling of fragments from a user-specified fragment source; c) computation of fragment trajectories with drag correction; d) physics-based 3D simulation of fragment impact, bounce and roll; e) use of trajectory-normal method for calculating fragment density; f) capability to track fragment impacts with a 3D structures wall and roof surfaces using collision detection algorithms; g) calculation of the expected number of penetrations into a building. The trajectory calculator has been verified with a range of established computer programs, and the bounce model has been compared against field test data with good agreement. The tool has been used to perform detailed, site-specific fragment risk analyses that account for unique fragmentation characteristics, uneven/non-uniform terrain, and the shielding of people or structures by natural geographical features or by other structures.</b>					
15. SUBJECT TERMS					
16. SECURITY CLASSIFICATION OF:			17. LIMITATION OF ABSTRACT  <b>SAR</b>	18. NUMBER OF PAGES  <b>36</b>	19a. NAME OF RESPONSIBLE PERSON
a. REPORT <b>unclassified</b>	b. ABSTRACT <b>unclassified</b>	c. THIS PAGE <b>unclassified</b>			

Outputs from the program are the PTN fragment density distribution over the terrain and the expected number of penetrations for each building. The PTN fragment density can be contoured to determine the hazardous fragment density area and distance. The building penetration data can be used for further risk analysis.

## FRAGMENT GROUP

A fragment group consists of one or more fragments with statistically identical characteristics, which include the mass, size, shape, aerodynamic properties, initial location and the explosion-induced velocity of the fragments. Each fragment group is defined in a reference frame that is usually different from the global coordinate system in which the buildings and terrain are defined. The reference frame for a fragment group can be stationary or moving. The latter allows, for example, the program to simulate explosion scenarios due to a space launch failure. Each simulation can contain one or more fragment groups.

During a Monte Carlo (MC) simulation, fragments are randomly sampled from each fragment group. All vector parameters are converted from the local reference frame to the global coordinate system, and the velocity of a moving reference frame is added to the explosion-induced velocities of individual fragments.

## FRAGMENT BALLISTIC TRAJECTORY

The translation and rotation of a ballistic fragment are described by the Newton-Euler equations:

$$m\ddot{\mathbf{r}}_c(t) = \sum \mathbf{f} \quad (1)$$

$$\mathbf{I}\dot{\boldsymbol{\omega}}(t) + \boldsymbol{\omega}(t) \times \mathbf{I}\boldsymbol{\omega}(t) = \sum \boldsymbol{\tau} \quad (2)$$

where  $m$  is the fragment mass,  $\mathbf{I}$  is the fragment moment of inertia matrix,  $\mathbf{r}_c$  is the translational position vector of the fragment center of mass,  $\boldsymbol{\omega}$  is the fragment angular velocity,  $\sum \mathbf{f}$  is the sum of all forces acting on the fragment, and  $\sum \boldsymbol{\tau}$  is the sum of all moments acting on the fragment. The forces acting on the fragment include the gravity and the drag. In a global coordinate system with the z-axis pointed upward, the vector of the gravity can be written as

$$\mathbf{f}_g = -mg \begin{Bmatrix} 0 \\ 0 \\ 1 \end{Bmatrix} \quad (3)$$

The drag can be written as

$$\mathbf{f}_d = -\frac{1}{2}C_D A \rho_{AIR} \|\mathbf{v}\| \mathbf{v} = -\frac{1}{2}C_D A \rho_{AIR} \|\dot{\mathbf{r}}_c\| \dot{\mathbf{r}}_c \quad (4)$$

where  $C_D$  is the coefficient of drag and  $A$  is the presented area of the fragment. Substituting Equations (3) and (4) into (1) gives

$$m\ddot{\mathbf{r}}_c + \frac{1}{2}C_D A \rho_{AIR} \|\dot{\mathbf{r}}_c\| \dot{\mathbf{r}}_c = \mathbf{f}_g \quad (5)$$

The fragment is assumed to be free of any moments while it is in free flight, and so the right-hand side term in Equation (2) is zero. The initial translational velocity of a fragment is the explosion-induced velocity plus the

velocity of the moving frame. The initial rotational velocity of a fragment is assumed to be zero, although the first impact with the terrain will usually introduce rotation. The equations for translation and rotation are integrated numerically.

## FRAGMENT BOUNCE ANALYSIS

### Bounce Equations

The bounce analysis determines the translational and rotational velocities of a fragment after it strikes the ground surface. The analysis is based on an impulse collision response algorithm described in (Mirtich, 1996). The basic assumptions of the analysis are: (1) the deformation of the fragment and the impacted surface are negligibly small so that they can be considered rigid; (2) Stronge's hypothesis applies; and (3) Coulomb's friction law holds.

The first assumption implies that the duration of the impact is infinitesimal and the force on the fragment is impulsive and instantaneously changes the velocity of the fragment. Since the fragment velocities are finite, the position of the fragment remains constant during the impact. Forces with finite magnitudes (such as gravity) have no effect over infinitesimal intervals, and so can be ignored in the bounce analysis.

While the first assumption idealizes the fragment and the impacted surface, in reality, there is always deformation associated with a force. The entire impact can be divided into two phases: a compression phase and a restitution phase. During the compression phase, the fragment pushes into the surface until the normal component of the fragment velocity at the contact point becomes zero; during the restitution phase, the fragment is pushed out by the restitution force. Let  $W_z(t_c)$  and  $W_z(t_r)$  be the work done by the normal component of impacted surface's resistance during the compression phase and the restitution phase, respectively, then Stronge's hypothesis states that

$$W_z(t_r) = -e^2 W_z(t_c) \quad (6)$$

where  $e$  is the coefficient of restitution, and the negative sign reflects the fact that the work done during the two phases have opposite signs.

In simple impact situations, such as for a spherical fragment, Stronge's hypothesis reduces to Newton's impact law:

$$u_z(t_r) = -e u_z(0) \quad (7)$$

where  $u_z(0)$  and  $u_z(t_r)$  are the normal component of the fragment velocities before and after the impact.

The Coulomb friction law can be expressed as

$$\begin{aligned} \mathbf{f}_t &= -\mu f_n \mathbf{u}_t / \|\mathbf{u}_t\| \quad \text{for } \mathbf{u}_t \neq 0 \\ \|\mathbf{f}_t\| &\leq \mu f_n \quad \text{for } \mathbf{u}_t = 0 \end{aligned} \quad (8)$$

where  $\mu$  is the coefficient of friction,  $\mathbf{u}_t$  is the tangential component of the fragment velocity at the impact point,  $f_n$  is the magnitude of the normal compression force, and  $\mathbf{f}_t$  is the tangential friction force. With the non-impulsive forces dropped, the Newton-Euler equations for the fragment in an impact can be written as

$$\mathbf{f}(t) = m\mathbf{a}(t) \quad (9)$$

$$\mathbf{r} \times \mathbf{f}(t) = \mathbf{I}\dot{\boldsymbol{\omega}}(t) + \boldsymbol{\omega}(t) \times (\mathbf{I}\boldsymbol{\omega}(t)) \quad (10)$$

where  $m$  and  $\mathbf{I}$  are the fragment mass and moment of inertia matrix,  $\mathbf{a}(t)$  is the translational acceleration at the center of mass,  $\boldsymbol{\omega}(t)$  is the angular velocity,  $\mathbf{f}(t)$  is the impact force, and  $\mathbf{r}$  is the offset vector from the center of mass to the impact point, as shown in Figure 1. It is noted that the ground surface needs not to be horizontal and the above equations are given in the body frame, a reference frame attached to the fragment.

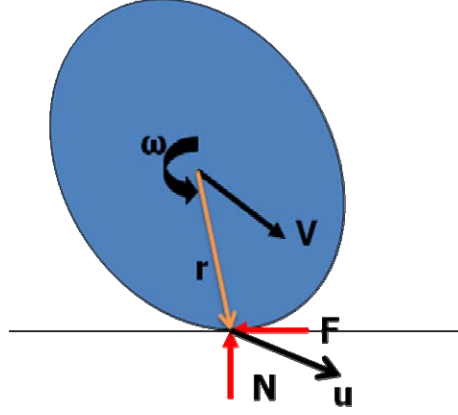


**Figure 1. Fragment impact on a surface**

The impact force and the resulting translational and rotational accelerations dominate the above equations, so the last term of Equation (10) can be dropped. With these simplifications, the above equations can be formally integrated over time to give

$$\mathbf{p}(t) = m\Delta\mathbf{v}(t) \quad (11)$$

$$\mathbf{r} \times \mathbf{p}(t) = \mathbf{I}\Delta\boldsymbol{\omega}(t) \quad (12)$$

where  $\Delta\mathbf{v}(t)$  and  $\Delta\boldsymbol{\omega}(t)$  are the changes in the translational and angular velocities, and  $\mathbf{p}(t)$  is the impact impulse:

$$\mathbf{p}(t) = \int_0^t \mathbf{f}(\tau) d\tau. \quad (13)$$

Time  $t$  has been used in the above formal derivation. For rigid body impact, the impact duration approaches zero and the impact forces become infinite. To avoid difficulties with these conditions, the impulse and velocities can be expressed as functions of a new impact parameter that monotonically increases during the course of the impact.

Denoting the new impact parameter by  $\lambda$ , Equations (11) and (12) can be written as

$$\Delta\mathbf{v}(\lambda) = \frac{1}{m}\mathbf{p}(\lambda) \quad (14)$$

$$\Delta\boldsymbol{\omega}(\lambda) = \mathbf{I}^{-1}[\mathbf{r} \times \mathbf{p}(\lambda)]. \quad (15)$$

The contact point velocity  $\mathbf{u}$  is given by

$$\mathbf{u}(\lambda) = \mathbf{v}(\lambda) + \boldsymbol{\omega}(\lambda) \times \mathbf{r} \quad (16)$$

and the change of  $\mathbf{u}$  can be written as

$$\Delta \mathbf{u}(\lambda) = \Delta \mathbf{v}(\lambda) + \Delta \boldsymbol{\omega}(\lambda) \times \mathbf{r} . \quad (17)$$

In the following derivation, the impact parameter  $\lambda$  is dropped from the variables unless ambiguity arises. Substituting Equations (14) and (15) into (17) gives

$$\begin{aligned} \Delta \mathbf{u} &= \frac{1}{m} \mathbf{p} - \mathbf{r} \times \mathbf{I}^{-1} (\mathbf{r} \times \mathbf{p}) \\ &= \left( \frac{1}{m} \mathbf{1} - \tilde{\mathbf{r}} \mathbf{I}^{-1} \tilde{\mathbf{r}} \right) \mathbf{p} \end{aligned} \quad (18)$$

where

$$\mathbf{1} = \begin{bmatrix} 1 & 0 & 0 \\ 0 & 1 & 0 \\ 0 & 0 & 1 \end{bmatrix} \quad \text{and} \quad \tilde{\mathbf{r}} = \begin{bmatrix} 0 & -r_3 & r_2 \\ r_3 & 0 & -r_1 \\ -r_2 & r_1 & 0 \end{bmatrix} \quad (19)$$

and  $r_1$ ,  $r_2$ , and  $r_3$  are the components of vector  $\mathbf{r}$ . Let

$$\mathbf{K} = \frac{1}{m} \mathbf{1} - \tilde{\mathbf{r}} \mathbf{I}^{-1} \tilde{\mathbf{r}} \quad (20)$$

then Equation (18) becomes

$$\Delta \mathbf{u} = \mathbf{K} \mathbf{p} . \quad (21)$$

Matrix  $\mathbf{K}$  is constant, symmetric and positive definite (Mirtich, 1996). The differential form of Equation (21) can be written as

$$\frac{d\mathbf{u}}{d\lambda} = \mathbf{K} \frac{d\mathbf{p}}{d\lambda} . \quad (22)$$

The above derivation is based on the Newton-Euler equations established in the body frame. It is more convenient to carry out the bounce analysis on a reference frame whose z-axis is aligned with the normal of the impacted surface and whose x- and y-axis fall on the impact surface. This reference frame is denoted the space frame.

Let  $\mathbf{R}$  be the transformation from the body frame to the space frame. Then in the space frame the vectors  $\mathbf{u}$  and  $\mathbf{p}$  can be written as

$$\hat{\mathbf{u}} = \mathbf{R} \mathbf{u} \quad (23)$$

$$\hat{\mathbf{p}} = \mathbf{R} \mathbf{p} . \quad (24)$$

Solving for  $\mathbf{u}$  and  $\mathbf{p}$  from Equations (23) and (24) and substituting them into Equation (22) gives

$$\frac{d\hat{\mathbf{u}}}{d\lambda} = \mathbf{R}\mathbf{K}\mathbf{R}^T \frac{d\hat{\mathbf{p}}}{d\lambda} = \hat{\mathbf{K}} \frac{d\hat{\mathbf{p}}}{d\lambda} \quad (25)$$

where

$$\hat{\mathbf{K}} = \mathbf{R}\mathbf{K}\mathbf{R}^T. \quad (26)$$

Since  $\mathbf{K}$  is positive definite,  $\hat{\mathbf{K}}$  is also positive definite, and Equation (25) can also be written as

$$\frac{d\hat{\mathbf{p}}}{d\lambda} = \hat{\mathbf{K}}^{-1} \frac{d\hat{\mathbf{u}}}{d\lambda}. \quad (27)$$

In the case where the tangential velocity is non-zero, that is,

$$\sqrt{\hat{u}_x^2 + \hat{u}_y^2} > 0 \quad (28)$$

the Coulomb friction law gives the force at the contact point as

$$\hat{\mathbf{f}} = \begin{pmatrix} -\mu \hat{f}_z \hat{u}_x / \sqrt{\hat{u}_x^2 + \hat{u}_y^2} \\ -\mu \hat{f}_z \hat{u}_y / \sqrt{\hat{u}_x^2 + \hat{u}_y^2} \\ \hat{f}_z \end{pmatrix} = \hat{f}_z \boldsymbol{\xi} \quad (29)$$

where

$$\boldsymbol{\xi} = \begin{pmatrix} -\mu \hat{u}_x / \sqrt{\hat{u}_x^2 + \hat{u}_y^2} \\ -\mu \hat{u}_y / \sqrt{\hat{u}_x^2 + \hat{u}_y^2} \\ 1 \end{pmatrix}. \quad (30)$$

If  $\sqrt{\hat{u}_x^2 + \hat{u}_y^2} = 0$ , then  $\boldsymbol{\xi}$  is undefined. This situation is termed *sticking* and requires special treatment. Sticking is divided into *stable sticking* and *unstable sticking*. In stable sticking, the tangential velocity becomes zero and remains zero from thereon. In non-stable sticking, the tangential velocity becomes zero only momentarily and sliding resumes after that.

The integration of the bounce equations is divided into the compression phase and the restitution phase. In the compression phase integration, the normal component of the fragment velocity  $\hat{u}_z$  at the contact point is used as the independent variable, and the tangent components of the contact point velocity,  $\hat{u}_x$  and  $\hat{u}_y$ , and the work  $W_z$  done by the normal component of the resistance force are the dependent variables. The integration is carried out until  $\hat{u}_z$  becomes zero.

In the restitution phase integration,  $W_z$  is used as the independent variable and the fragment velocity at the contact point is the dependent variable. The integration is carried out until  $W_z$  reaches a value determined from Stronge's hypothesis. The reader is referred to (Mirtich, 1996) for details of the integration process.

The outcome of the restitution phase integration is the bounce velocity  $\hat{\mathbf{u}}$  at the contact point. The velocity change,  $\Delta\hat{\mathbf{u}}$ , is the difference between the bounce velocity and the initial velocity. The total impulse that acts on the fragment during the impact can be calculated from Equation (27) as

$$\hat{\mathbf{p}} = \hat{\mathbf{K}}^{-1} \Delta\hat{\mathbf{u}} \quad (31)$$

in the space frame, or

$$\mathbf{p} = \mathbf{R}^T \hat{\mathbf{p}} = \mathbf{R}^T \hat{\mathbf{K}}^{-1} \Delta\hat{\mathbf{u}}. \quad (32)$$

in the body frame.

The change in the angular velocity is then calculated from (15) as

$$\Delta\boldsymbol{\omega} = \mathbf{I}^{-1} (\mathbf{r} \times \mathbf{p}). \quad (33)$$

The change in the center of mass velocity can be calculated from Equation (14) as

$$\Delta\mathbf{v} = \frac{1}{m} \mathbf{p} \quad (34)$$

in the body frame. With  $\Delta\boldsymbol{\omega}$  and  $\Delta\mathbf{v}$  known, the exit angular velocity and translational velocity can be calculated:

$$\boldsymbol{\omega}(t_f) = \boldsymbol{\omega}(t_0) + \Delta\boldsymbol{\omega} \quad (35)$$

$$\mathbf{v}(t_f) = \mathbf{v}(t_0) + \Delta\mathbf{v} \quad (36)$$

The exit angular velocity and translational velocity are used as the initial conditions for the next phase of airborne trajectory of the fragment.

### Comparison with Experimental Data

Comparison of the bounce model was made with the experimental data presented in (Fletcher & Bowen, 1968) based on the ending bounce distance of concrete blocks. In the experiment more than 500 objects were dropped on smooth flat ground (a graded airstrip on an alluvial plain) from a truck traveling at speeds ranging from 10 to 60 mph and the distances traveled by the objects were measured. The objects included stones (1.3—116 lb), ordinary concrete building blocks, concrete filled building blocks, and several types of animals. Our comparison study was made only with the filled concrete building blocks since their weights (55.0-56.5 lb), shape (cuboid), and size (7.5×7.7×15.5 inches) were well defined.

In the analytic simulation, the blocks were dropped in random orientations at the height of the truck bed (2.6 feet) and with a horizontal velocity ranging from 15 ft/s to 100 ft/s, mimicking the test conditions. The coefficient of restitution and the coefficient of friction were not available from the test. Instead, the restitution and friction coefficients used in ACTA's range safety software were employed in the simulation. The coefficient of restitution is a function of the normal impact speed, as shown in Figure 2. The coefficients of friction are constant, with 0.9 for soft surface and 0.5 for hard surface.



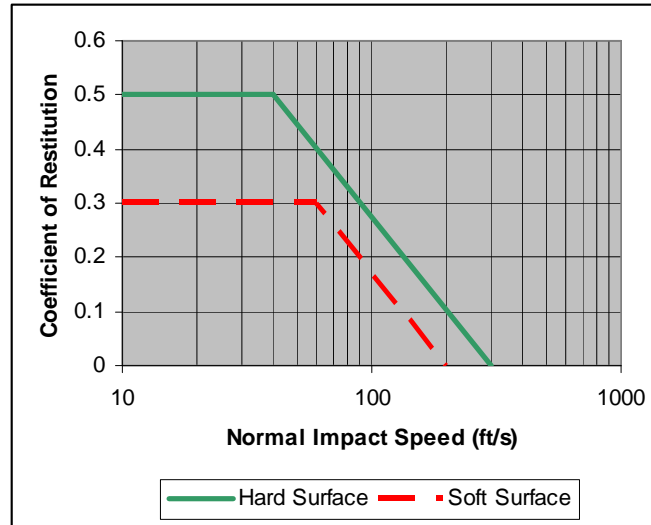


**Figure 2. Coefficient of Restitution.**

Figure 3 shows sample fragment trajectories. All the trajectories in the figures correspond to the same initial fragment height and velocity. The initial orientation of the fragment is randomly sampled and is responsible for the variations in the trajectories after the first impact. It is noted that many of the fragments reach a height above the initial drop height of 2.6 feet. This is due to the conversion of the momentum associated with the horizontal velocity into vertical momentum, and is one of the differences between a spherical object and a non-spherical object.

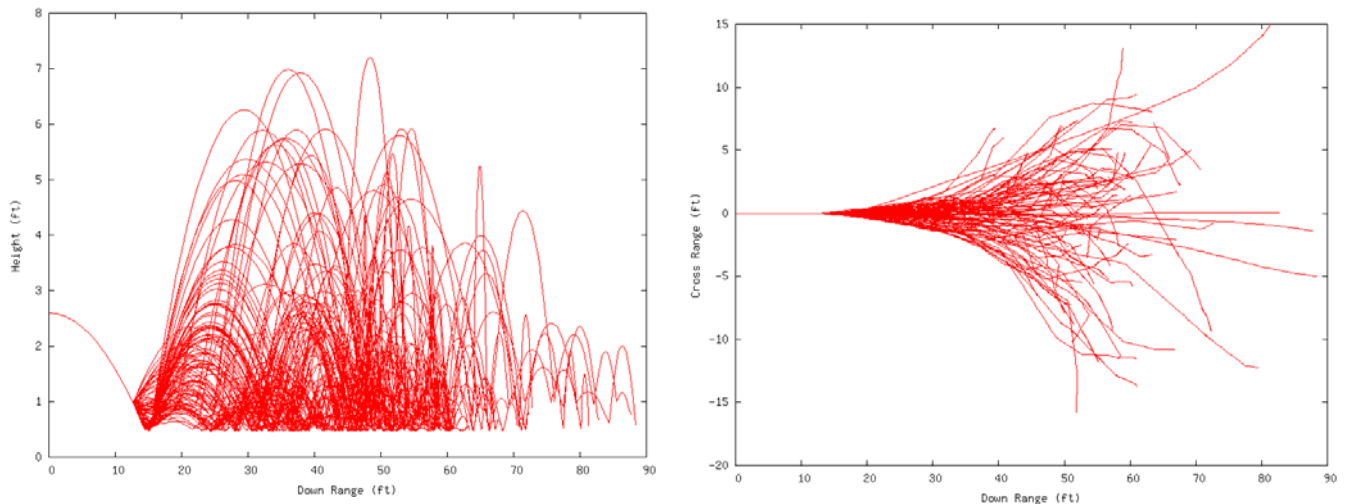


**Figure 3. Sample fragment trajectories (height vs. downrange & cross range vs. down range).**

**Error! Reference source not found.** compares the test and simulated fragment travel distances. In the figure, the solid and hollow squares represent the mean test distances for the solid and the hollow blocks respectively. The regression line and the lines for the  $\pm 1$  standard error for the test data are plotted in solid and dashed lines. The simulation results with soft and hard surfaces are plotted in error bars (mean  $\pm 1$  standard error). As one can see, the predicted distances are higher than the test results in most cases but are still within the range of error of the test.

The over prediction with the hard surface is more pronounced than with the soft surface, which is expected considering the fact that the hard surface model is intended for concrete pavement. Figure 5 shows a sequence of 3D snapshots from a bounce simulation

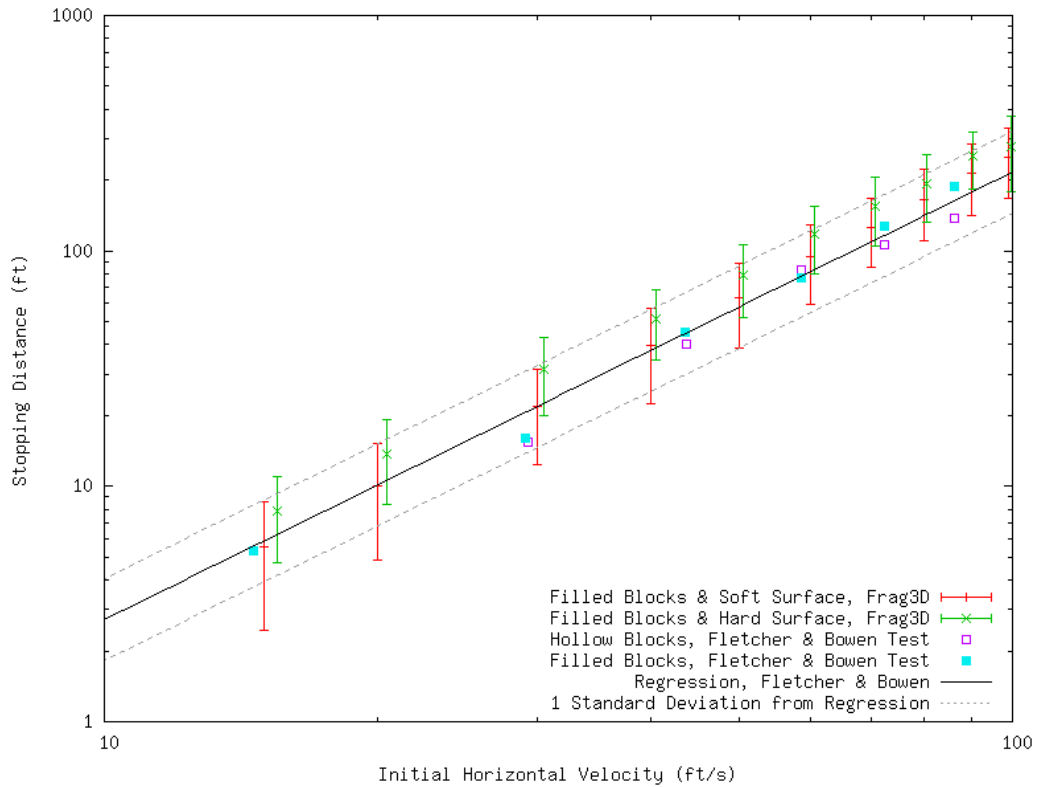


**Figure 4. Comparison with experimental stopping distance.**

## PSEUDO TRAJECTORY NORMAL FRAGMENT DENSITY

Fragment density (number of fragment impacts per unit area) is a common used quantity to measure the hazard of fragment impact. Depending on the situations, the fragment density can be calculated with a number of different methods, and the results from these methods may not be comparable. In field tests, for example, fragments in gridded areas are picked up after they have stopped. In simple numerical simulations, the number of fragment impacts is usually counted. Neither method is able to distinguish the difference between a high angle fragment that falls almost vertically and a low angle fragment that has a flat, near ground trajectory. In both of the two methods, a fragment flying past a grid area 3 feet above ground will have no contribution to the fragment density for the grid area, even though a person standing inside the grid area can potentially be hit by the fragment. The pseudo trajectory normal (PTN) fragment density is an alternative method that is used to correct these problems.

The PTN fragment density accounts for the height  $H_r$  of the impact receiver of interest, and its calculation is based on the intersection of the fragment trajectory with an associated volume generated by vertically extruding a grid area on the ground surface to a height equal to  $H_r$ , as shown in **Error! Reference source not found.** for a triangular grid area. The PTN fragment density for a particular ground triangle is defined as

$$D_{PTN} = \sum \frac{1}{A_{PTN}} \quad (37)$$

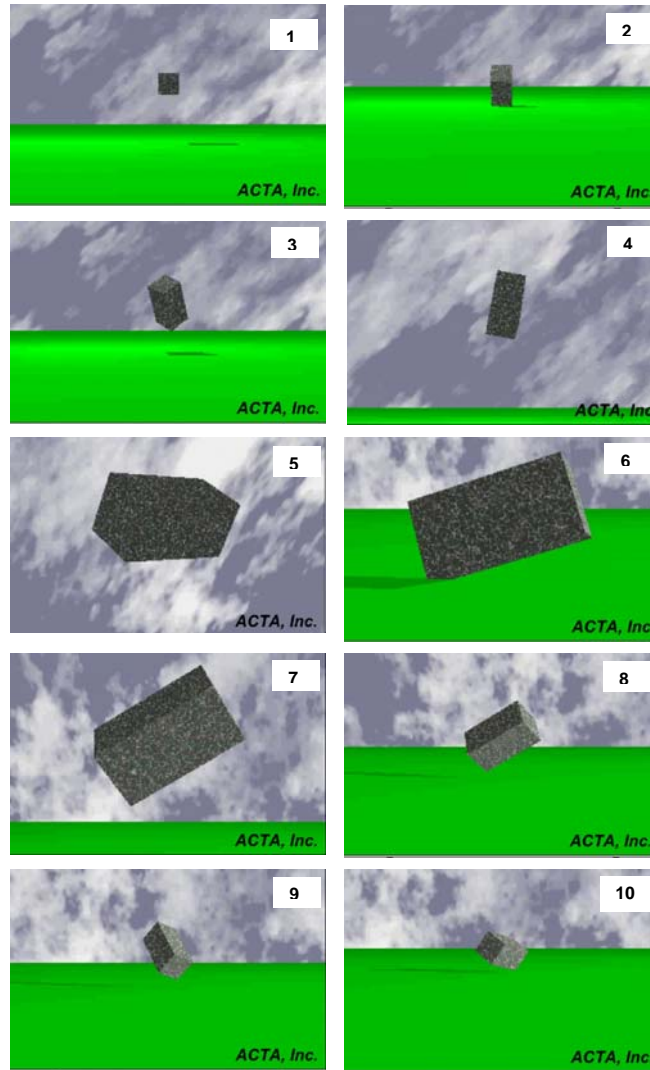


**Figure 5. A sequence of frames from a fragment bounce simulation.**

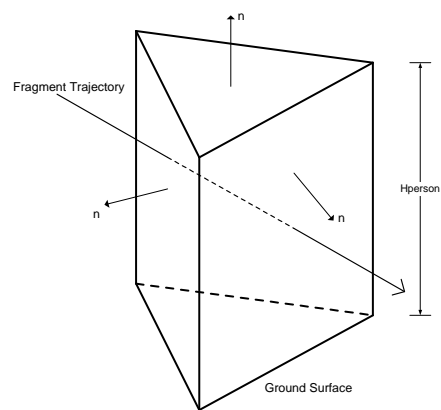


**Figure 6. Pseudo Trajectory Normal Fragment Density Calculation.**

where the summation is over all fragments whose trajectories intersect with the associated volume of the ground triangle, and  $A_{PTN}$  is the PTN-projected area of the associated volume with respect to a fragment trajectory. The PTN-projected area for an associated volume is the sum of the PTN-projected areas of the faces of the prism:

$$A_{PTN} = \sum A_{PTN}^{(i)} \quad (38)$$

where the summation is over all faces of the prism, and

$$A_{PTN}^{(i)} = \begin{cases} -A_i \mathbf{n}_i \cdot \mathbf{v}_f / \|\mathbf{v}_f\|, & \text{if } \mathbf{n}_i \cdot \mathbf{v}_f < 0 \\ 0, & \text{if } \mathbf{n}_i \cdot \mathbf{v}_f \geq 0 \end{cases} \quad (39)$$

where  $A_i$  and  $\mathbf{n}_i$  are the area and unit (outward) normal vector of  $i$ -th face of the prism, respectively, and  $\mathbf{v}_f$  is the fragment velocity vector.

It is noted that, if all the fragments fall vertically, the PTN method gives the same fragment density as dividing the number of fragments that hit a ground triangle by the area of the triangle. The two methods diverge for fragments falling in slanted trajectories. The more the trajectories are slanted, the larger the difference. As the trajectories become horizontal, the number of fragment impacts on the ground triangle becomes zero, but the PTN still gives a reasonable fragment density that can be used to evaluate the hazard of fragment impact on exposed people.

Figure 7 shows the PTN fragment density due to a simulated explosion of a jet assisted takeoff solid rocket motor used in the launch of target planes. The motor is tilted up and pointed to the east to northeast direction. The preferential dispersion of the fragments in the radial, axial forward and axial rearward directions give the butterfly-shaped fragment density contour.

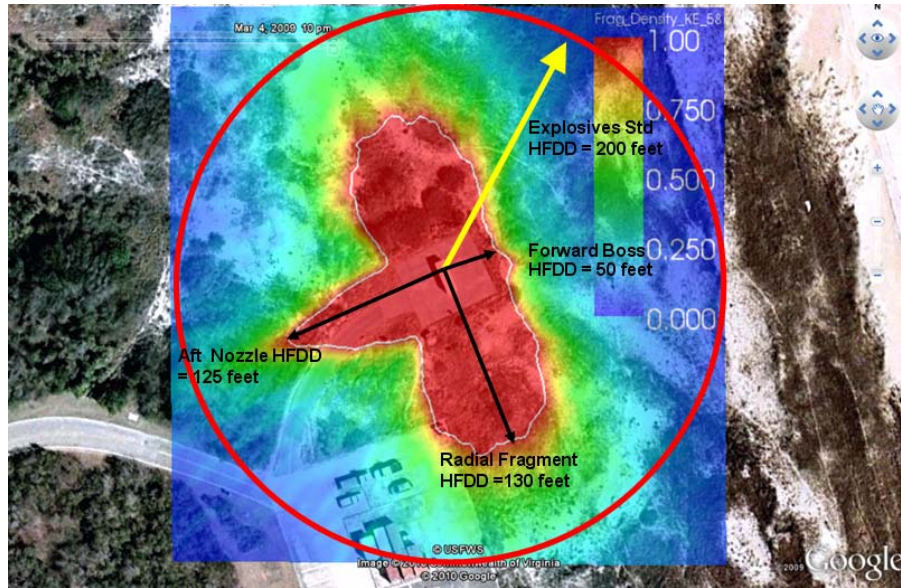


**Figure 7. PTN fragment density due to a simulated explosion of a jet assisted takeoff motor.**

## FRAGMENT IMPACT ON 3D OBJECTS

The PTN fragment density discussed above is appropriate for evaluating the fragment impact hazard for people since the height of an average person is used as the characteristic height in the calculation. While the same calculation can be done for 3-dimensional objects, such as buildings and storage tanks, difficulties arise due to the potentially wide variation in the heights of these entities. Additionally, we may also be interested in the penetration of fragments into buildings, which is affected by construction of the walls and roof of the buildings as well as the impact angle. Under such a circumstance, a more appropriate approach is to determine the impacts on each 3D object directly during a simulation. To do this, a 3D object is modeled with triangle mesh, as shown in Figure 8, and the impact of a fragment with the object is determined through collision detection.

Figure 9 shows the results of a simulated early time launch failure. The trajectory plot includes only a randomly selected subset of all the trajectories generated in the simulation. The buildings are colored by the expected number of fragment penetrations, with blue representing no penetration and red the highest number of penetrations. Fragment bounce is not included in this particular simulation. Figure 10 shows a simulation of the 1997 Delta II explosion.

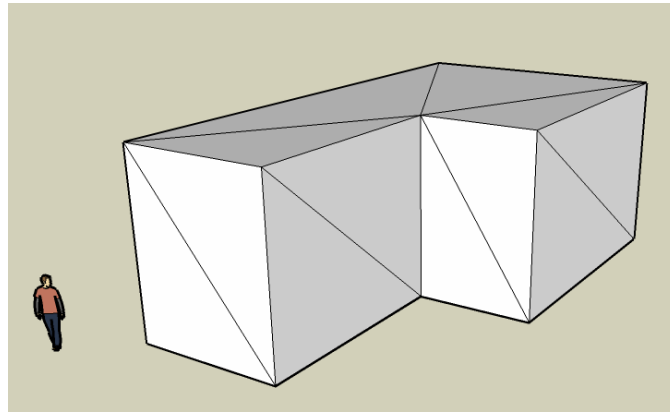


**Figure 8. 3D Model of a Building.**

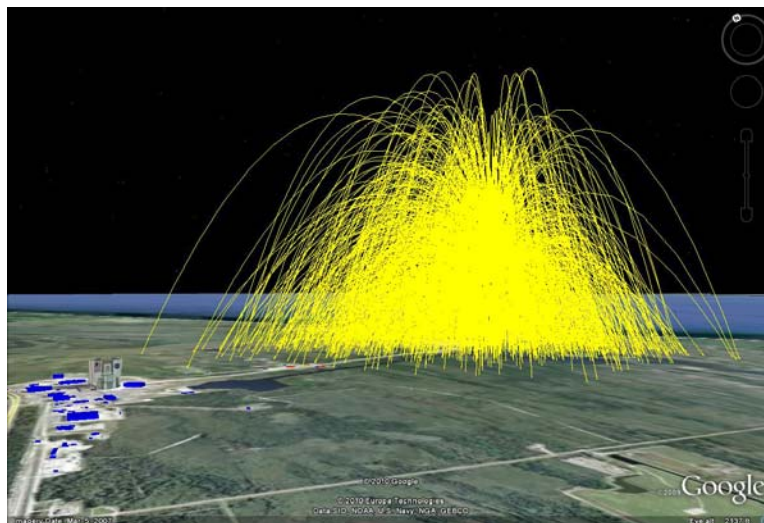


**Figure 9. Fragment impact in a simulated early time launch failure.**





**Figure 10. Simulation of the 1997 Delta II explosion.**

## SUMMARY

DebrisHaz performs detailed 3D fragment throw simulation, computes pseudo trajectory fragment density on meshed terrain, and outputs expected numbers of fragment impacts and penetrations for buildings. It provides a useful means to perform site-specific analysis in supplement to the regular Q-D analysis, taking into account of the information unique to the project. The program is still under active development, and more features will be added to it. DebrisHaz will be incorporated as a module in the HAZX Hazard Tool to simplify its use by end users

## REFERENCES

Chrostowski, J. D., et al (2010), HAZX Part1: An Explosion Hazard Assessment Tool, 2010 Department of Defense Explosives Safety Board Seminar, Portland, Oregon.

Fletcher, E. R., & Bowen, I. G. (1968). Blast-Induced Translational Effects. *Annals of NY Academy of Sciences* , 152 (1), 378-403.

Mirtich, B. V. (1996). *Impulse-Based Dynamic Simulation of Rigid Body Systems*. PhD Thesis, University of California, Berkeley, CA.

# **DebrisHaz 3D Fragment Throw Simulation to Determine Fragment Fragment Hazards and Consequences**

**Author/Co-Author**

**Wenshui Gan/Jon Chrostowski**  
**ACTA, Inc.**

**2010 DDESB Explosives Safety Seminar**  
**Portland, OR**

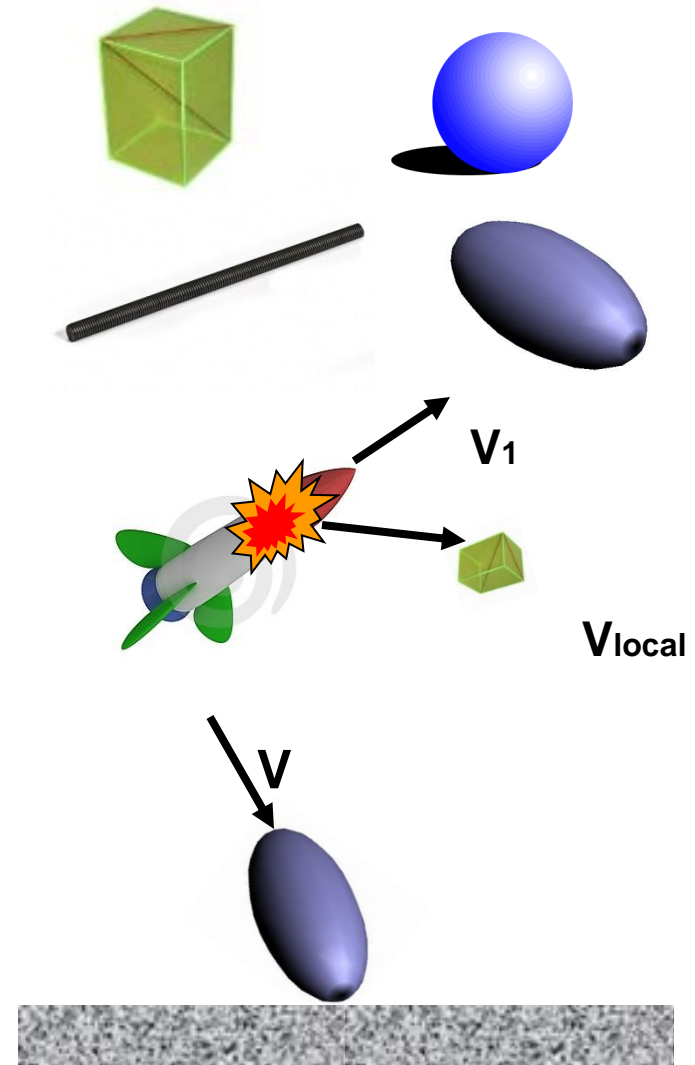
***July 15, 2010***





# Fragments and Fragment Groups

- DebrisHaz considers 3D fragments and point mass fragments.
  - *Shapes include spheres, cuboids, ellipsoids, rods*
- A fragment group contains fragments with statistically identical properties (*random but w/ same mean and distribution on size, mass, velocity, etc.*)
- Each fragment group is defined in a local reference frame, which can be stationary or moving (as in the explosion of an in-flight rocket).
- Fragments are randomly sampled from fragment groups and their interactions with the terrain and buildings are tracked.



# Free-Flight Trajectory

---

## Newton-Euler equations

$$m\ddot{\mathbf{r}}_c(t) = \sum \mathbf{f}$$

$$\mathbf{I}\dot{\boldsymbol{\omega}}(t) + \boldsymbol{\omega}(t) \times \mathbf{I}\boldsymbol{\omega}(t) = \sum \boldsymbol{\tau}$$

The integration of the N-E equations is carried out numerically until the fragment impacts the ground, at which point the calculation is switched to a bounce analysis.

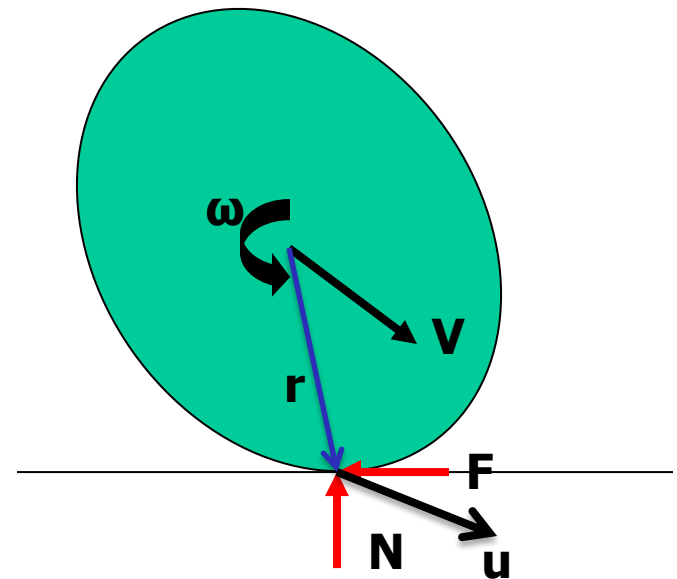
# Fragment Bounce Analysis

---

- **Basic Assumptions**
  - *A fragment has shape and size*
  - *Deformation of fragment and impacted surface is negligible.*
  - *Stronge's restitution hypothesis applies*
    - Work done by restitution force is a fraction of the work done by the compression force.
    - For spherical fragment, this reduces to Newton's impact law.
  - *Coulomb's friction law applies.*

# Fragment Bounce Analysis

- Mass
- Moment of inertia
- Forces during impact:
  - *Normal reaction,  $N$*
  - *Friction,  $F$*
- Velocities
  - *Translational velocity at C.G.*
  - *Rotational velocity*



# Fragment Bounce Analysis

Newton-Euler equations:

$$\mathbf{f}(t) = m\dot{\mathbf{v}}(t)$$

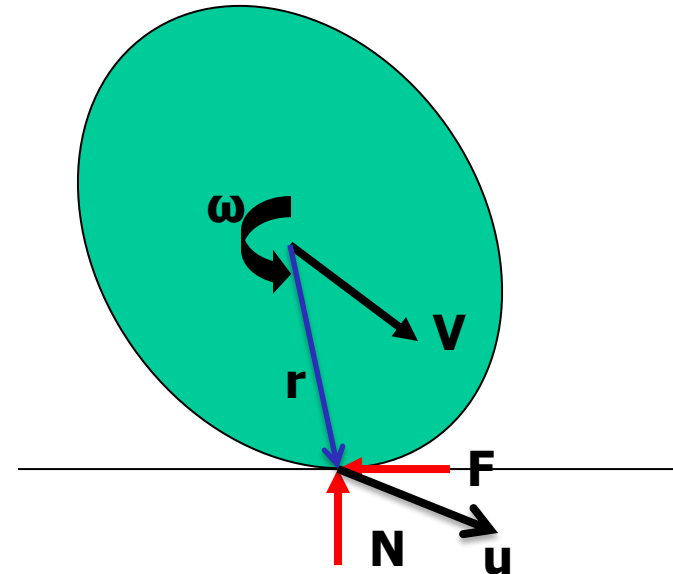
$$\mathbf{r} \times \mathbf{f}(t) = \mathbf{I}\dot{\boldsymbol{\omega}}(t) + \boldsymbol{\omega}(t) \times (\mathbf{I}\boldsymbol{\omega}(t))$$

Contact point velocity:

$$\mathbf{u} = \mathbf{v} + \boldsymbol{\omega} \times \mathbf{r}$$

Contact force:

$$\mathbf{f} = \begin{pmatrix} -\mu f_z u_x / \sqrt{u_x^2 + u_y^2} \\ -\mu f_z u_y / \sqrt{u_x^2 + u_y^2} \\ f_z \end{pmatrix} \quad \text{for } u_x^2 + u_y^2 > 0$$



# Fragment Bounce Analysis

---

After applying the assumption of impulsive impact:

$$\mathbf{p} = m\Delta\mathbf{v}$$

$$\mathbf{r} \times \mathbf{p} = \mathbf{I}\Delta\boldsymbol{\omega}$$

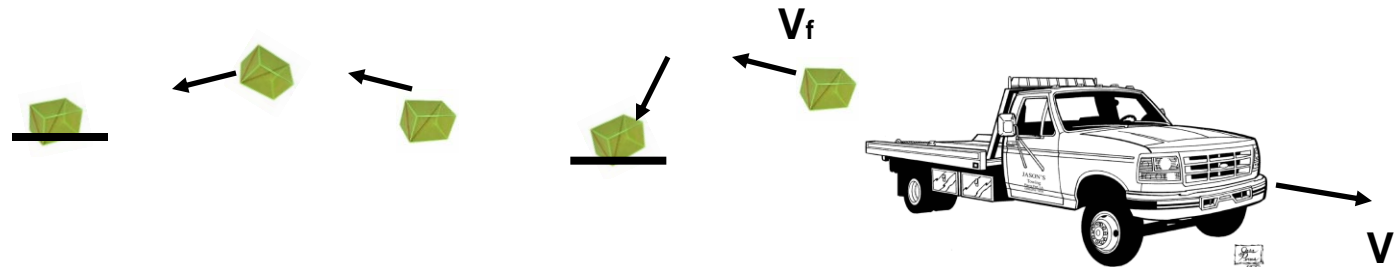
$$\Delta\mathbf{u} = \Delta\mathbf{v} + \Delta\boldsymbol{\omega} \times \mathbf{r}$$

$$\mathbf{p} = \mathbf{f}\Delta t$$

Integration of the above equations give the bounce velocities.

# Fragment Bounce Test Comparison

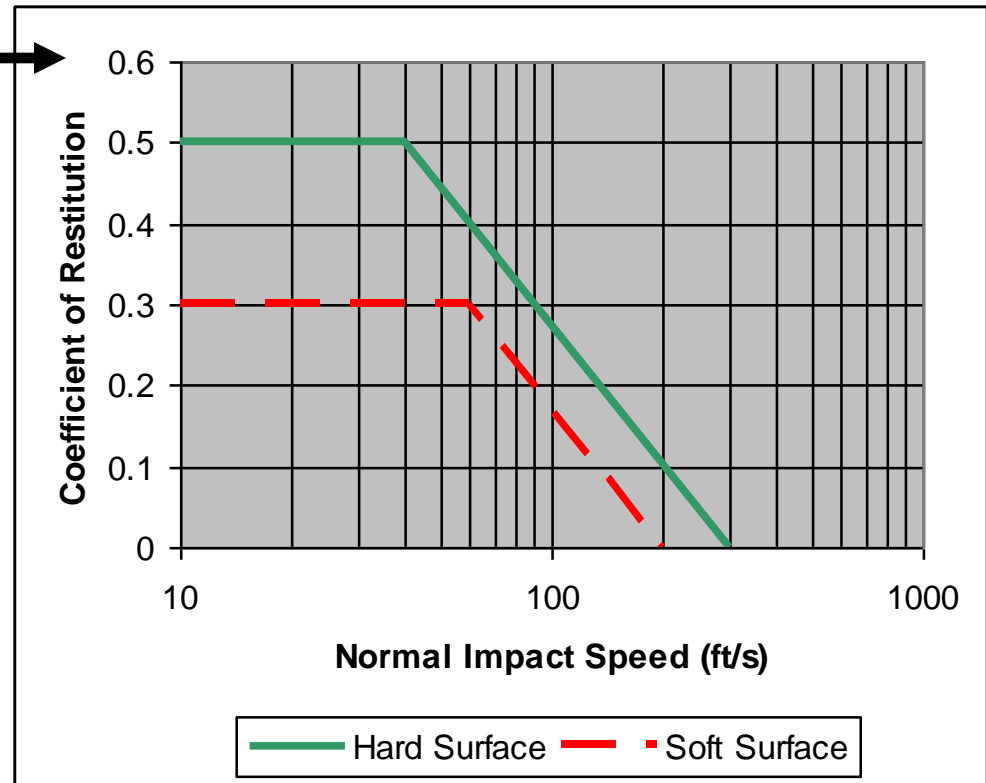
- Test data by Fletcher & Bowen (1968),
  - *7.5"x7.5"x15.5" hollow & solid concrete blocks*
  - *Dropped from the bed of a truck moving at speeds ranging from 10 to 60 mph on a graded airstrip*
  - *Travel distance measured*
- Simulation
  - *Solid concrete block modeled as cuboid*
  - *Drop height 2.6 ft (height of truck bed)*
  - *Horizontal velocity 15 ft/s to 100 ft/s*





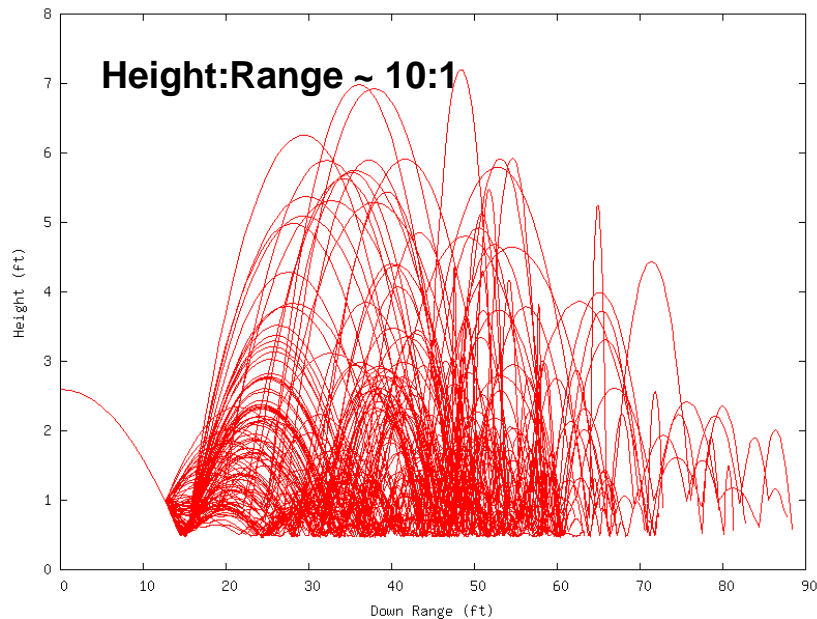
# Fragment Bounce Test Comparison

- Restitution coefficients were not available from test. Instead, data in ACTA's range safety software were used.
- Coefficient of friction is 0.9 for soft surface and 0.5 for hard surface.
- Simulations were done for both hard and soft surfaces.

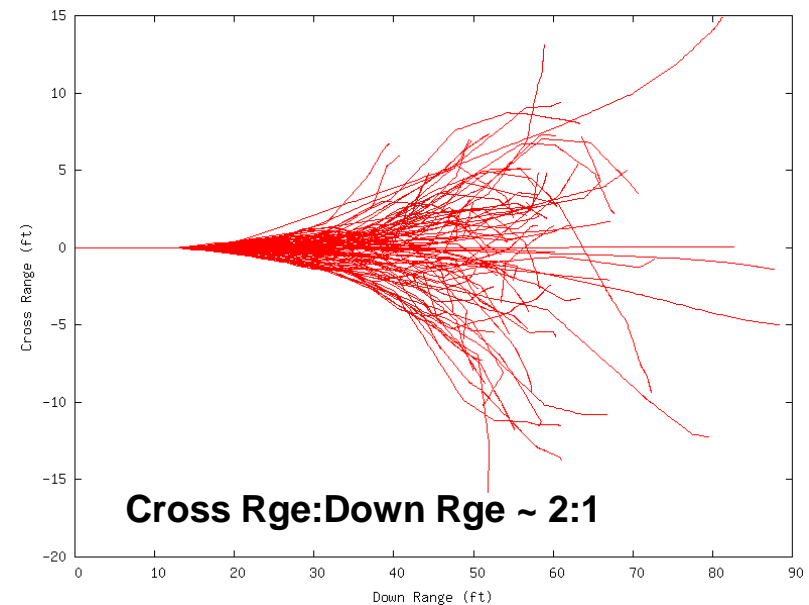


# Fragment Bounce Simulation Samples

## Sample fragment trajectories with bounce



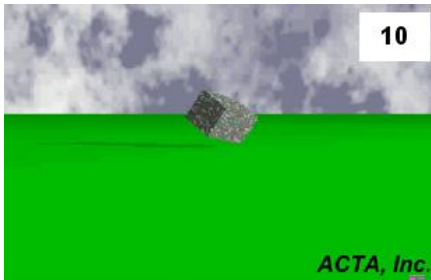
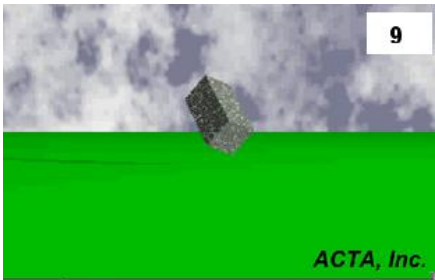
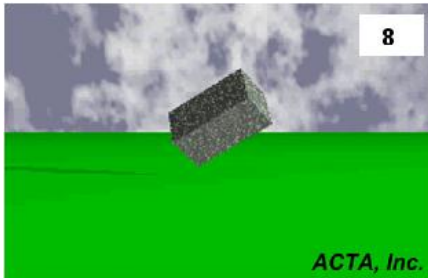
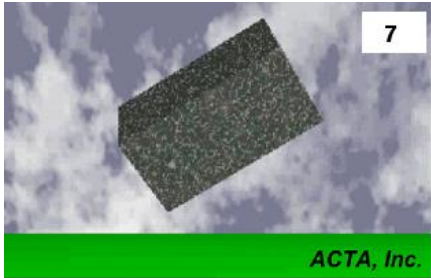
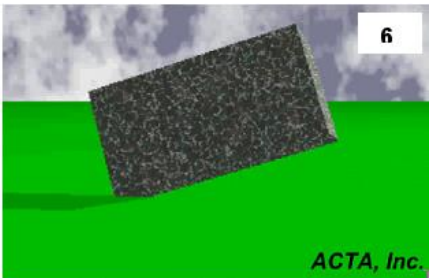
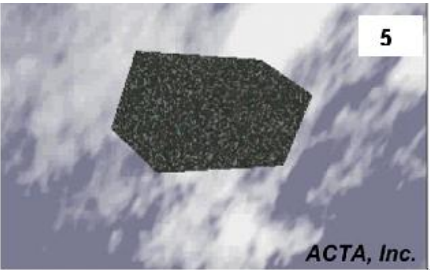
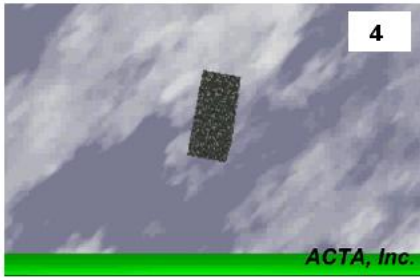
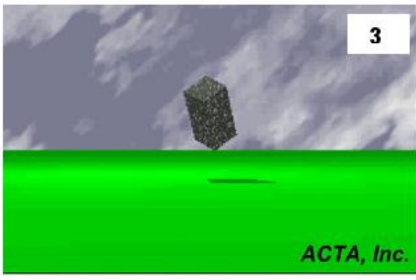
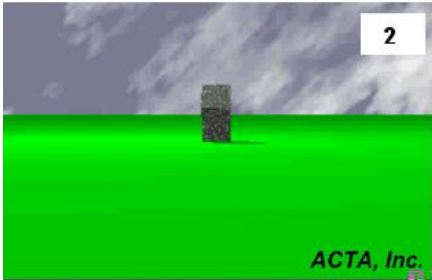
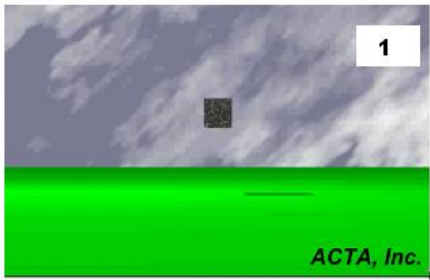
**Side view**



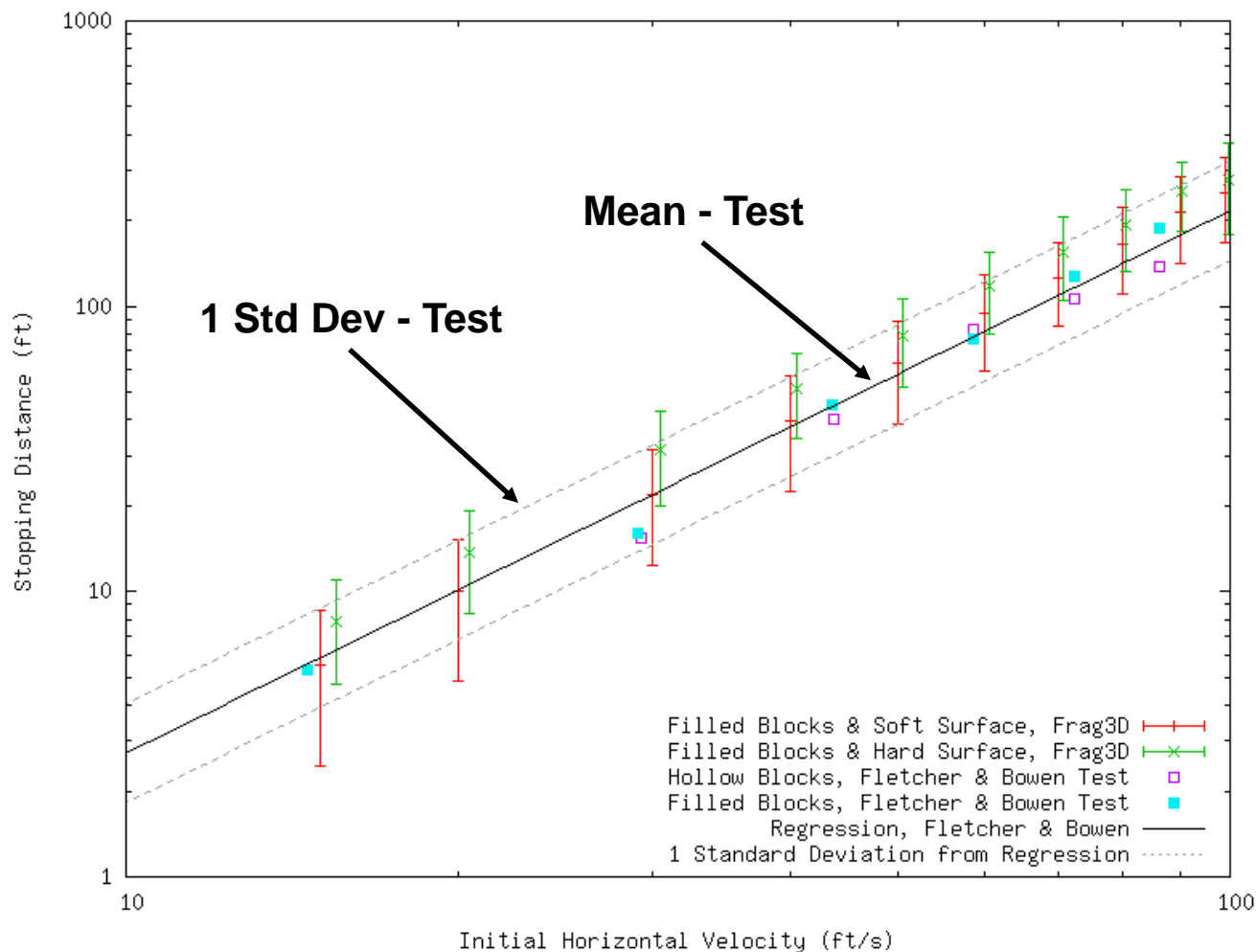
**Plan view**

Note: All fragments in the plots have the same initial velocity and height but their takeoff orientations are random.

# Snapshots of the 3D Bounce Model

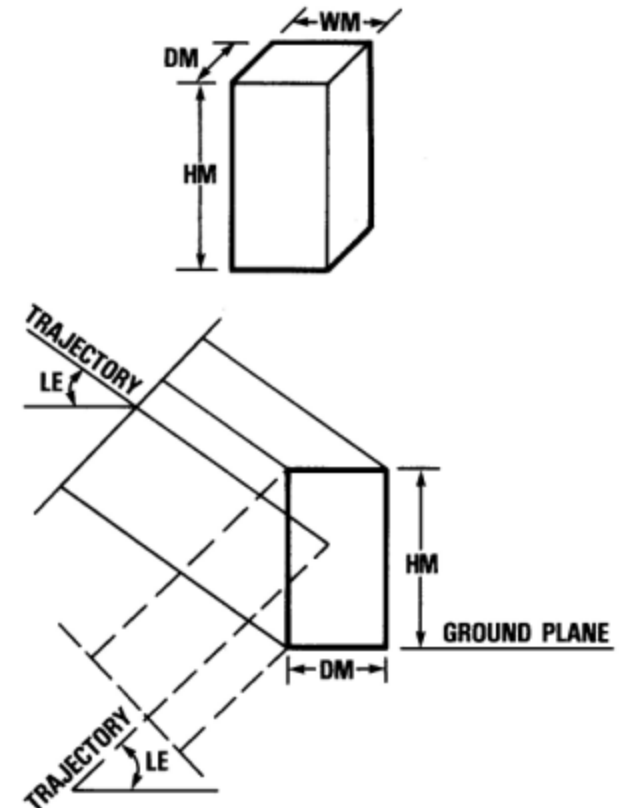


# Fragment Bounce Test/Simulation Comparison



# Pseudo Trajectory Normal Fragment Density

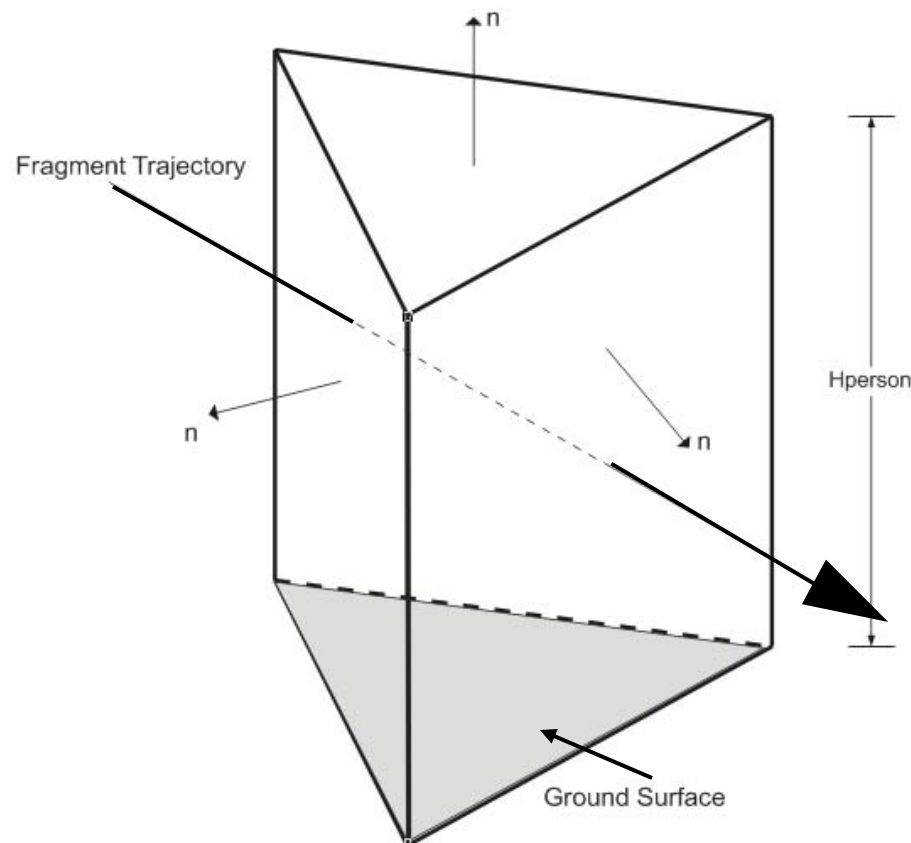
- Hazardous fragment density is used in determining equivalent protection.
- Different methods exist for the calculation of fragment density.
  - *Some methods may underestimate the real impact risk for low-flying fragments with flat trajectories.*
  - *Calculation based on PTN corrects this problem.*



20

# Pseudo Trajectory Normal Fragment Density

- In DebrisHaz the ground surface is meshed with triangles.
- The triangles are extruded to the height of a typical person.
- Each hazardous fragment whose trajectory intersects with the extruded volume of a triangle contributes to the fragment density of the triangle.

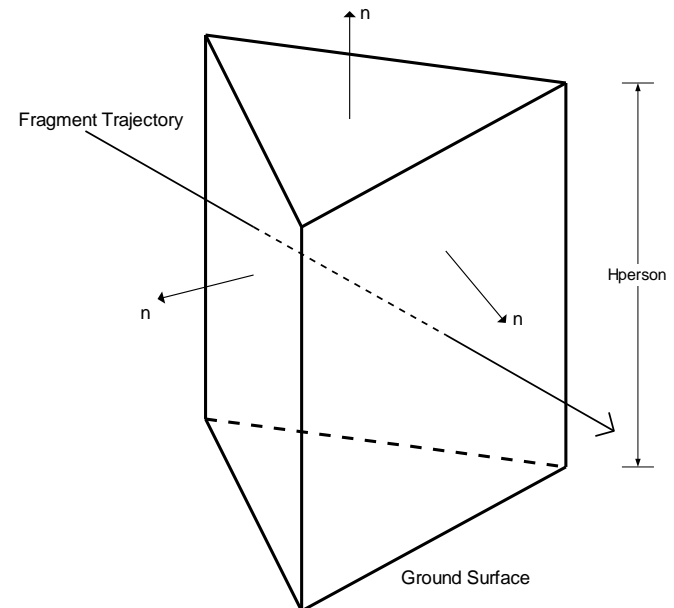


# Pseudo Trajectory Normal Fragment Density

- The contribution of a fragment to the PTN fragment density is the inverse of the area resulting from projecting the extruded volume onto a plane that is normal to the trajectory of the fragment.

$$D_{PTN} = \sum \frac{1}{A_{PTN}} \quad A_{PTN} = \sum A_{PTN}^{(i)}$$

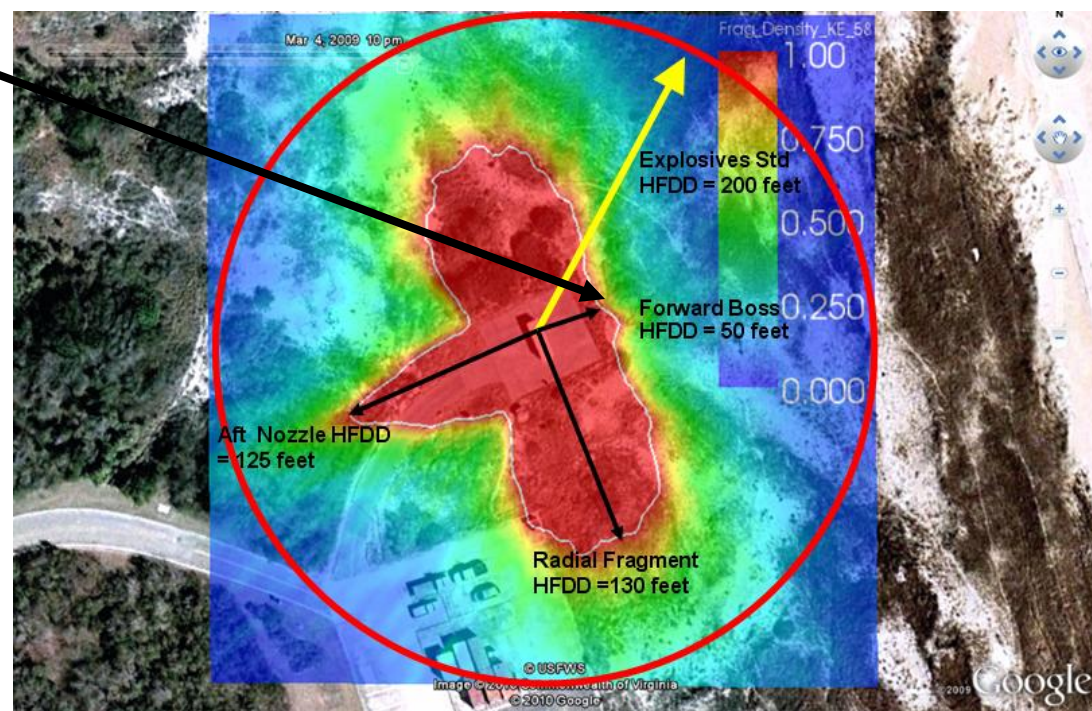
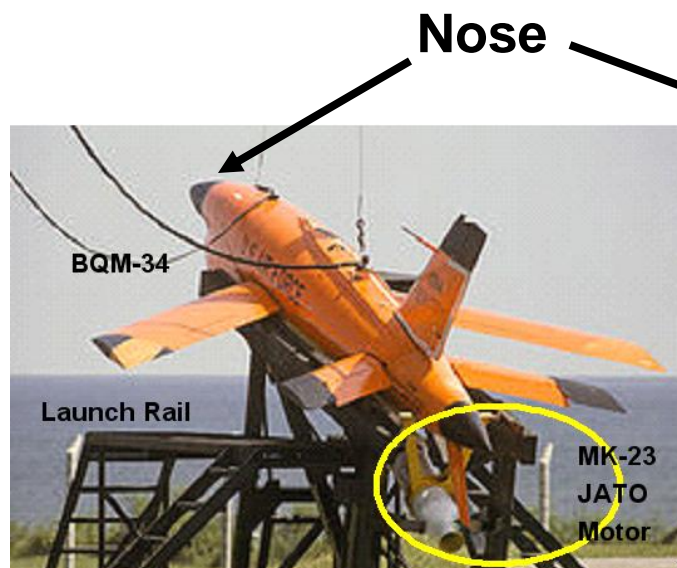
$$A_{PTN}^{(i)} = \begin{cases} -A_i \mathbf{n}_i \cdot \mathbf{v}_f / \|\mathbf{v}_f\|, & \text{if } \mathbf{n}_i \cdot \mathbf{v}_f < 0 \\ 0, & \text{if } \mathbf{n}_i \cdot \mathbf{v}_f \geq 0 \end{cases}$$





# Example of PTN Fragment Density Calculations

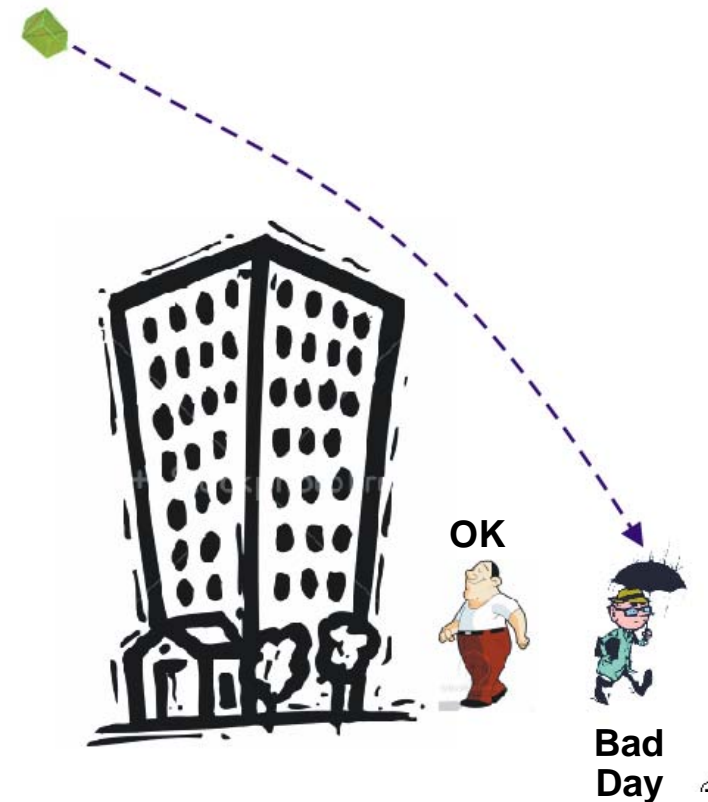
- Simulated on-rail explosion of a winged target vehicle with a solid rocket motor assist at takeoff.
- Asymmetric shape of the hazardous fragment density contour results from preferential fragment flight out pattern.





# Fragment Impact on Buildings

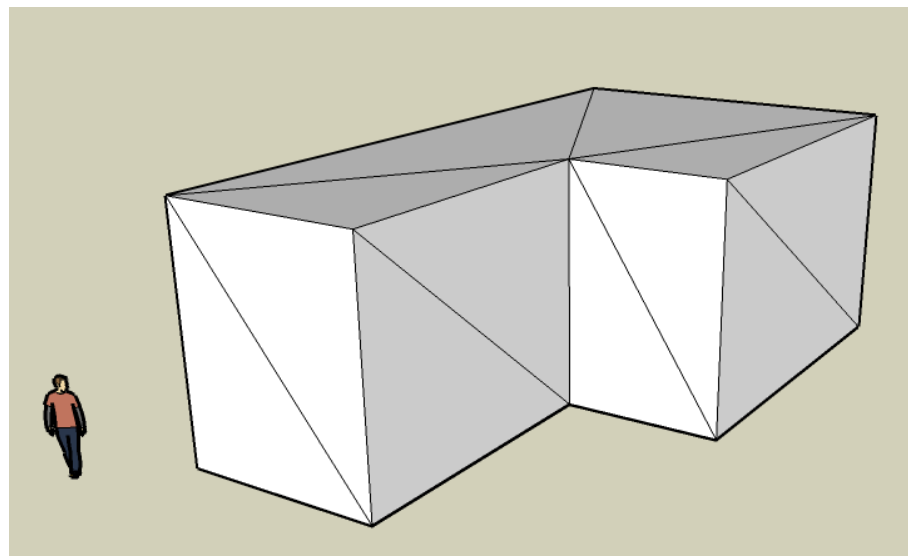
- PTN fragment density is suitable for evaluating the risk of fragment impact on people in the open.
  - *Intervening buildings and other objects may provide protection*
- It is not suitable for predicting building impacts and consequences to occupants:
  - *Wide variation in building heights*
  - *Wide variation in impact resistance, both within a building (wall/roof) and among different buildings.*
  - *Blocking of fragments by one building on another*
- The DebrisHAZ physics-based tool addresses all these issues



# Fragment Impact on Buildings

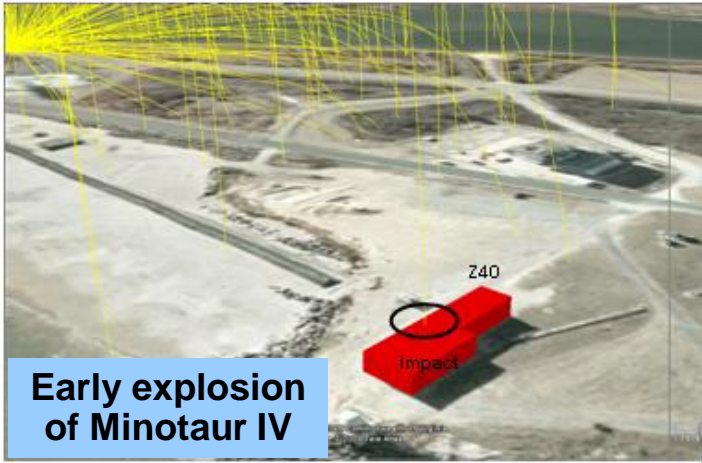
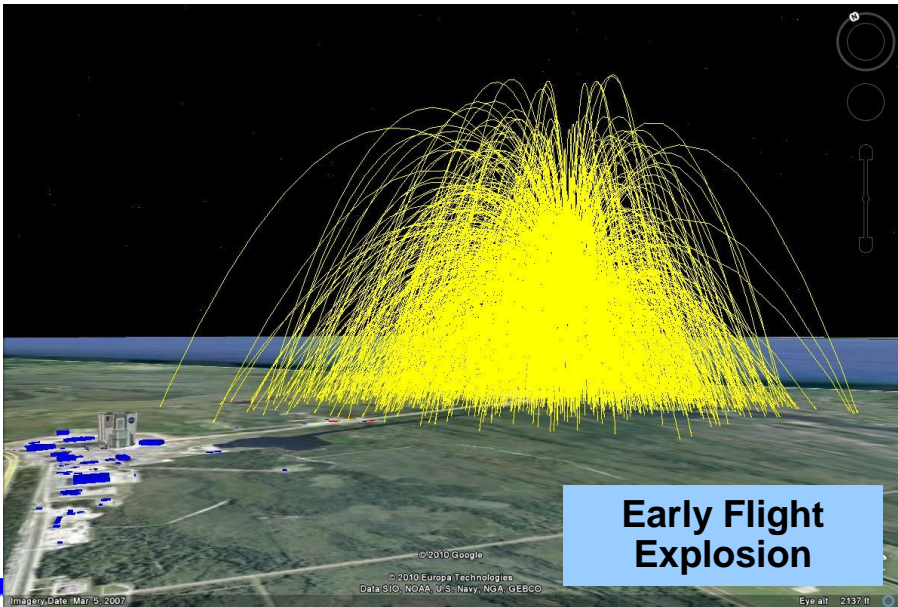
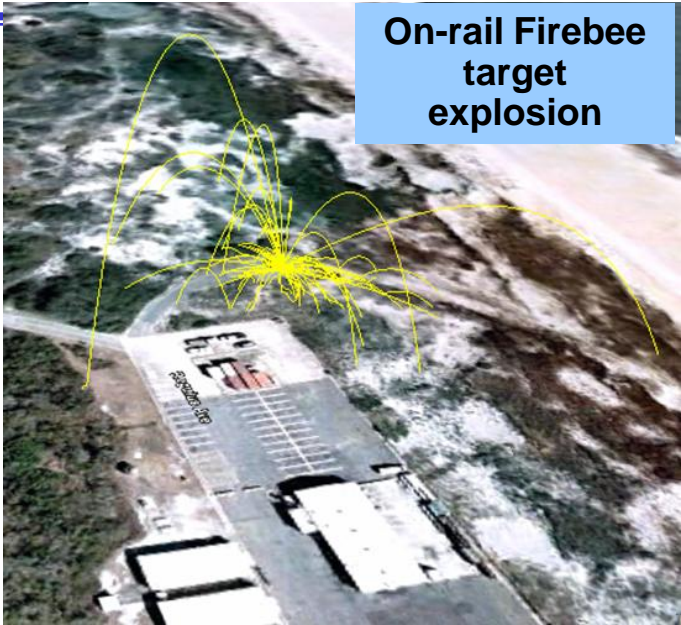
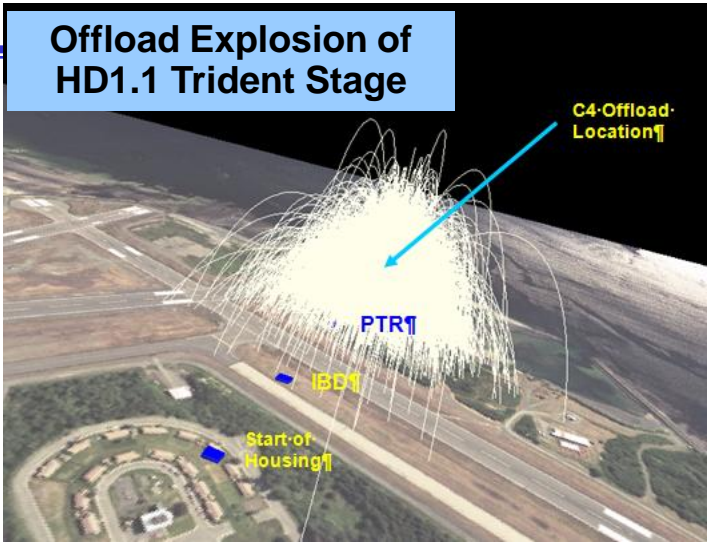
*(This process is being automated in HAZX)*

- 3D models are created using Google Sketchup™.
  - *Footprint are extruded upward to height*
  - *Surfaces are meshed*
- Structural properties are assigned to walls, roof & windows.
  - *Properties used to determine kinetic energy of penetration*
- DebrisHaz determines fragment impacts on building surfaces & uses KE & frag area to predict whether it penetrates or not



- Residual fragment KE is used to predict injury to building occupants

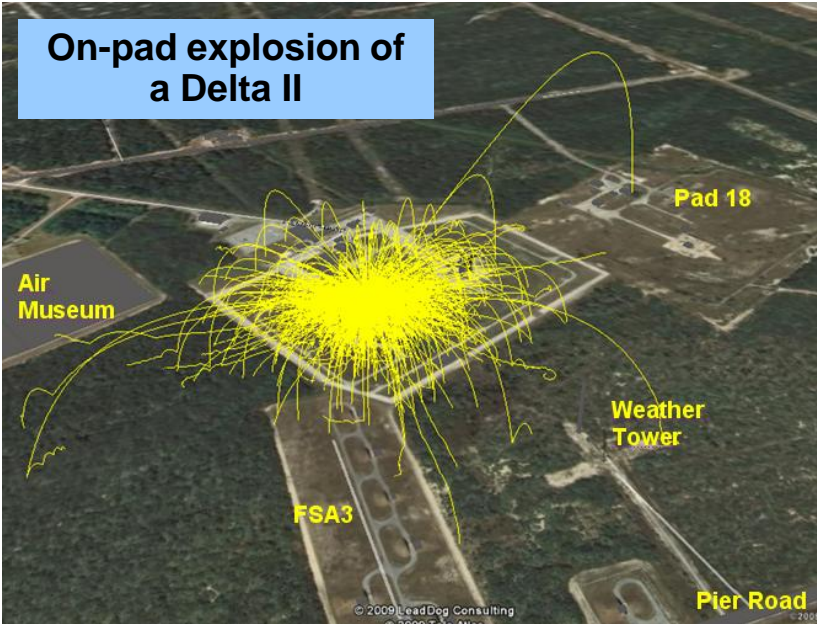
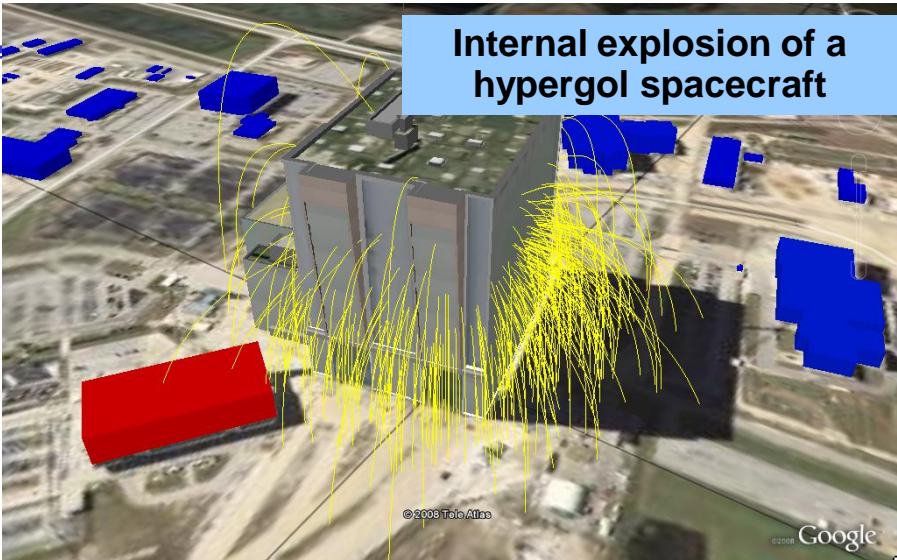
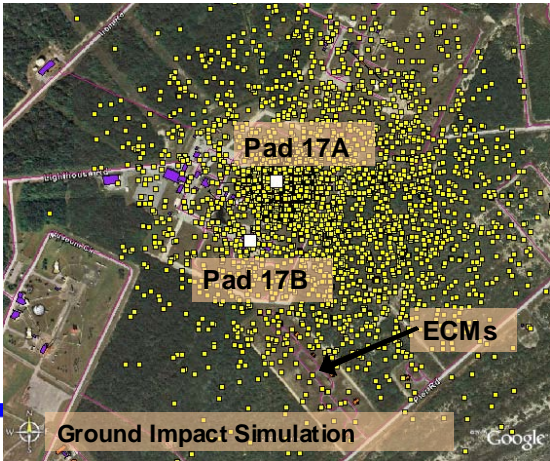
# Examples of DebrisHaz Analyses





# Examples of DebrisHAZ Analyses

1997 T+14 explosion  
of a Delta II



# Summary

- DebrisHaz is used to perform detailed 3D fragment throw simulations when site-specific siting issues are important
  - *Tracks trajectories of all fragments & calculates intersects with other objects (e.g., bldgs, barriers) and the ground surface*
  - *Considers terrain and the bounce of fragments*
  - *Performs a PTN analysis to determine hazardous fragment density*
  - *Calculates impacts and penetrations of buildings and effects on occupants*
- DebrisHaz is being incorporated underneath HAZX in order to automate the entire process
  - *Users will be able to perform detailed fragment throw analyses on their own*